Published in final edited form as:
Acta Histochem. 2011 February ; 113(2): 150–155. doi:10.1016/j.acthis.2009.09.006.

PRDM16 Expression in the Developing Mouse Embryo

Kristin H. Horn, **Dennis R. Warner**, **M. Michele Pisano***, and **Robert M. Greene**
University of Louisville Birth Defects Center, Department of Molecular, Cellular and Craniofacial Biology, School of Dentistry Louisville, Kentucky 40292

SUMMARY

PRDM16 is a member of the PR domain-containing protein family and is associated with various disease states including myelodysplastic syndrome and adult T cell leukemia, as well as developmental abnormalities such as cleft palate. It is also known to act as a regulator of cell differentiation. Expression analysis of *PRDM16* is limited, especially within the developing embryo. The current study evaluated the temporal and spatial localization of *PRDM16* during early mouse development (embryonic days 8.5–14.5). *PRDM16* was first detected on E9.5 in a limited number of tissues and by E14.5, was expressed in a broad range of developing tissues including those of the brain, lung, kidney, and gastrointestinal tract. The expression pattern is consistent with a role for *PRDM16* in the development of multiple tissues. Collectively, these studies are the first to characterize the expression of the *PRDM16* gene during early murine development.

Keywords

embryo; development; MEL1; PRDM16; transcription factor

INTRODUCTION

PRDM16 (also known as MDS1/EVI1-like gene 1 [MEL1] or PFM13) was discovered from studies of (1;3)(p36;q21)-positive myeloid leukemias where it was found to be inappropriately expressed and was hypothesized to promote hyperproliferation (Mochizuki et al. 2000; Nishikata et al. 2003a). Most of the published studies to date on *PRDM16* have focused on its role in these specific leukemias and have resulted in the emergence of the notion that *PRDM16* is a tumor suppressor (Yoshida et al. 2004; Shing et al. 2007). *PRDM16* belongs to a 17- (human) or 16- (mouse) member family of PR (PRDI-BF1 and RIZ1 homologous) domain containing proteins (PRDMs). It is a 140 kDa protein that, in addition to the PR domain, includes two DNA binding domains of either 7- or 3-C_2H_2 type zinc fingers. The *PRDM16* gene is located on chromosome 1p36.3 and shares 56% sequence homology and a similar domain structure to *MDS1/EVI1* (Mochizuki et al. 2000). *MDS1/EVI1*, in turn, is similar in structure to the known oncogene, *EVI1*. The PR domain was first identified based on its homology to a 100 amino acid sequence shared between positive

***Author to whom correspondence should be addressed:** M. Michele Pisano, Ph.D. Department of Molecular, Cellular and Craniofacial Biology University of Louisville, ULSD 501 South Preston Street, Suite 301 Louisville, KY 40292 Phone: (502) 852-1962 FAX: (502) 852-8309 pisano@louisville.edu.

regulatory domain I binding factor 1 (PRDI-BF1; PRDM1) and retinoblastoma-interacting zinc finger protein (RIZ; PRDM2) (Keller and Maniatis 1991; Buyse et al. 1995). It shares 20–30% identity with the SET domains (Suvar3–9, Enhancer-of-zeste, Trithorax) found on a class of histone methyltransferases. *PRDM16* has two known splice variants: a 170 kDa isoform and a short form (s*PRDM16*) truncated at the amino terminus resulting in the absence of most of the PR domain (Nishikata et al. 2003b).

Recent studies have demonstrated that *PRDM16* is highly expressed in brown adipose tissue (BAT) and that forced expression in preadipocytes leads to induction of the BAT cell program (Seale et al. 2007). This is accomplished, in part, by formation of a transcriptional complex that includes CtBP-1 and CtBP-2 that represses the transcription of genes associated with formation of white adipose tissue (Kajimura et al. 2008). Thus, in addition to its proposed role in cell proliferation, *PRDM16* can drive certain tissue-specific differentiation. Given its size and complex domain structure, it is likely that *PRDM16* forms complexes with numerous proteins, which may, in part, explain its diverse functions. We have previously demonstrated that *PRDM16* forms a complex with various Smad proteins, important mediators of TGFß and BMP signaling (Warner et al. 2007). While the functional role of this interaction is unclear, regulation of TGFß-induced gene expression through modulation of the strength and/or extent of the TGFß response may be mediated by *PRDM16*/Smad interactions. Because Smad 3 was identified as a *PRDM16* binding protein in orofacial tissue, we have proposed a role for this protein in development of this tissue, and specifically, the secondary palate (Warner et al. 2007). In support of this hypothesis is the observation that a missense mutation of *PRDM16* results in an isolated cleft palate in mice (Bjork et al. 2006).

To date, studies investigating the expression of *PRDM16* have been limited. Mochizuki et al. (2000) reported that *PRDM16* is expressed in the uterus, fetal kidney, and leukemia cells with the t(1;3) translocation. Moreover, *PRDM16* expression has also been described in adult human heart, brain, placenta, lung, liver, skeletal muscle, kidney, pancreas, peripheral blood, and bone marrow (Lahortiga et al. 2004). Van Campenhout et al. (2006) described *PRDM16* expression in neural crest cells migrating into the second branchial arch, the otic vesicle, the brain, the retinal pigment epithelium of eye, the heart, and the kidney at various stages of *Xenopus* development. More recently, we observed *PRDM16* expression in the heart, brain, liver, limb bud, palate, nasal septum, and upper lip within mid- to late- staged (E13.5–E14.5) mouse embryos (Warner et al. 2007). Delineation of the role of *PRDM16* during embryonic development necessitates knowledge of its spatial and temporal patterns of expression. The purpose of the current study was to assess the spatial and temporal localization of *PRDM16* during early and midgestational development of the mouse.

MATERIALS AND METHODS

Animals

ICR mice (Harlan Laboratories; Indianapolis, IN) were utilized for these studies. The use of animals for these experiments was approved by the University of Louisville Institutional Animal Care and Use Committee. Mice were maintained on a 12-hour light/dark cycle in an American Association for Accreditation of Laboratory Animal Care (AAALAC) approved facility at the University of Louisville. For timed matings, two females were housed overnight with a single, mature male and the presence of a vaginal plug the following morning was taken as evidence of copulation. This time point was designated as embryonic day 0.5 (E0.5). Embryos were collected on each embryonic day between E8.5 and E12.5, and on E14.5 and processed for *in situ* hybridization analysis as described below.

Riboprobe Synthesis

The generation of sense and antisense riboprobes to *PRDM16* have been described previously (Warner, *et al*., 2007). Briefly, a 508 bp fragment of murine *PRDM16* was cloned into plasmid pSPT-18 (Roche Diagnostics, Indianapolis, IN). The resulting plasmid was linearized with either EcoRI (for antisense probe) or HindIII (sense probe) and riboprobes synthesized with the DIG RNA labeling kit (Roche Diagnostics) followed by a series of lithium chloride precipitations to remove free nucleotides. Probe yields were determined via a NanoDrop ND-1000 Spectrophotometer (NanoDrop Technologies, Wilmington, DE) and probe quality was assessed by agarose gel electrophoresis. Only transcripts demonstrating a single, compact band were utilized for these experiments.

Sectional *In situ* Hybridization

Mouse embryos of the appropriate gestational age were collected into cold calcium/magnesium-free phosphate buffered saline (PBS) (Gibco Invitrogen Corp., Gaithersburg, MD) and crosslinked overnight in fresh 4% (w/v) paraformaldehyde (Polysciences, Warrington, PA) / PBS. Following crosslinking, embryos were processed through a series of overnight sucrose washes (30% [w/v] sucrose (Fisher Scientific, Pittsburgh, PA) / PBS then 1:1 30% [w/v] sucrose/PBS, and finally Optimum Cutting Temperature compound [OCT, Sakura Finetek, Torrence, CA]), frozen in OCT, and stored at −80 °C until sectioned. Frozen serial sections, eight to twelve microns (8–12 um) thick, were prepared using a cryostat (Leica CM1900; Leica Microsystems Nussloch GmbH, Nussloch, Germany), collected onto RNase-free glass slides (VWR, Media, PA), and dried overnight at room temperature to ensure adherence of the sections. Slide-mounted sections were then crosslinked with 4% (w/v) paraformaldehyde/PBS and endogenous peroxidases were quenched with 6% (v/v) hydrogen peroxide (Fisher Scientific). Tissue sections were permeabilized with 1 μg/ml proteinase K (Roche Diagnostics) for 15 minutes. Digestion was stopped by incubation for 10 minutes in 2 mg/ml glycine (Fisher Scientific). Sections were then washed with PBT (PBS + 0.1% (v/v) Tween-20 [Fisher Scientific]) and again crosslinked in 4% (w/v) paraformaldehyde/0.2% (v/v) glutaraldehyde (Fisher Scientific) / PBT for 15 minutes at room temperature. Sections were then prehybridized at 65°C for 1 hour (50% formamide; 5X SSC, pH 4.5; 50 μg/ml yeast tRNA, 1% SDS; 50ug/ml heparin, all from Sigma Chemical Co., St. Louis, MO) and then incubated overnight at 65°C in the same solution containing 500–1000 ng/ml DIG-labeled riboprobe. Sections were then washed, blocked for one hour in 5% sheep serum (Sigma Chemical Co.), and again incubated overnight at 4°C with alkaline phosphatase-labeled anti-digoxigenin antibody (0.375 units/ml, Roche Diagnostics). Riboprobe-specific hybridization was detected by exposing sections to (188 μg/ml NBT / 94 μg/ml BCIP (nitro blue tetrazolium chloride/5-Bromo-4-chloro-3-indolyl phosphate) (Roche Diagnostics) and 2 mM tetramisole (Sigma Chemical Co.) for three to four days at in the dark at room temperature. Color development was quenched by washing with PBS (pH 5.5), and sections mounted in Biomedia™Crystal/Mount (Electron Microscopy Sciences, Hatfield, PA). For each embryonic day analyzed, at least two embryos were fully sectioned and 5–6 slides from each embryo were analyzed with either the sense- or antisense-PRDM16 riboprobe, with similar patterns of expression observed.

Image acquisition

Images were taken with a Nikon DXM1200F digital camera controlled by a computer running ACT-1 acquisition software and mounted on a Nikon Eclipse E600 microscope (Nikon, Inc., Melville, NY). All images were collected under similar lighting and are presented without digital alteration.

RESULTS

To gain insight into the role that *PRDM16* may play in embryonic development, we evaluated the temporal and spatial localization of *PRDM16* mRNA during early and midgestational development of the mouse (E8.5–E14.5).

Embryonic day 9.5

While expression of *PRDM16* mRNA was not observed by *in situ* hybridization until E9.5, we detected *PRDM16* by RT-PCR in earlier embryos (E8.5, data not shown). This is likely because the level of expression on E8.5 may be below the limit of detection by *in situ* hybridization. On E9.5, however, expression of *PRDM16* was observed predominately in the neuroepithelium lining the telencephalic vesicle (TV), within the mesenchyme of the first branchial arch (BA1), and in the dorsal aspect of the somites (Som) (Fig. 1, panels B–E). No signal was detected when a *PRDM16* sense riboprobe was used (Fig. 1, panel A).

Embryonic day 10.5

As development proceeds, expression of *PRDM16* is found in an increasing number of tissues. On E10.5 expression remained in the telencephalic vesicle (TV) and was also found in the neuroepithelium of the hindbrain (HB) and in the optic stalk (OS) (Fig. 2C). Expression continued in the first branchial arch (BA1) and was seen to have expanded into the mesenchyme of the second and third branchial arches (BA2 and BA3, respectively, Fig. 2D) and into the epithelium of the stomadeal roof (Stom) (Fig. 2D). The limb bud (LB) (Fig. 2E) and the facio-acoustic preganglion complex (FACP) (Fig. 2F) were also *PRDM16*-positive.

Embryonic day 11.5

By E11.5, expression of *PRDM16* was found in the medial and lateral nasal processes (MNP and LNP, respectively) (Fig. 3C) and continued to be present in the first branchial arch (BA1) (Fig. 3C and 3D). *PRDM16* expression was seen in the developing liver (L) and heart (Ht) (Fig. 3E), as well as in the trigeminal ganglion (TNG) (Fig. 3F) and the vertebral region of the sclerotome (VR) (Fig. 3G).

Embryonic day 12.5

On E12.5, *PRDM16* expression continued in the brain, specifically in the neuroepithelium lining the third ventricle (3^{rd} V, Fig. 4B). In the orofacial region, *PRDM16* was found in Meckel's cartilage (MC) (Fig. 4C) and the future nasal septum (NS) (Fig. 4D). In addition, *PRDM16* was also expressed in the dorsal root ganglia (DRG) (Fig. 4E), lung epithelium (LUE) (Fig. 4F), liver (L), stomach (STOM) (Fig. 4G) and duodenum (D)(Fig. 4H).

Embryonic day E14.5

On E14.5, there was widespread expression of *PRDM16*. The brain (Br) maintained *PRDM16* expression (Fig. 5B). In the orofacial region, *PRDM16* was expressed in the oral epithelium (OE), vestibulocochlear ganglion (VIII), trigeminal ganglion (TNG), and submandibular glands (SMG) (Figs. 5C and 5D). Additional tissues in which *PRDM16* expression was detected included the pancreatic primordium (Pan), testes (Te), kidney (Ki), and adrenal gland (AG) (Fig. 5E). Expression continued to be seen in the developing lung (Lu) and dorsal root ganglia (DRG) (Fig. 5F). Expression was also detected in the cartilage primordia of the developing rib (CPR, Fig. 5F). In the developing limbs (limb bud, LB), *PRDM16* expression was restricted to the perichondrial region (Fig. 5G, arrows). Finally, expression in the eye was found in the pigment layer of the retina and in the developing lens (PLR and Lens, respectively, Fig. 5H).

DISCUSSION

The expression of *PRDM16* was first detected by *in situ* hybridization on E9.5. Between E9.5 and E14.5, the expression pattern of *PRDM16* quickly expanded to include many types of tissue. There was consistent expression in the developing brain and other neural tissue, branchial arches, and nascent lung throughout the gestational period examined. In addition, *PRDM16* was expressed in the developing liver, gut, and eye. Based upon previous analyses (Lahortiga et al. 2004), much of this pattern of expression persists into adulthood. Because *PRDM16* is a putative transcription factor capable of interacting with many different proteins, it may have unique functions, depending upon the cell type in which it is expressed and thus may be critical for the modulation of multiple signaling pathways. We have recently demonstrated that PRDM16 interacts with multiple members of the Smad family of nucleocytoplasmic proteins that transmit extracellular signals from TGFßs and BMPs to the nucleus (Warner et al. 2007). Therefore it is possible that *PRDM16* modulates these two pathways in embryonic development. Recently, it was shown that *PRDM16* is necessary for differentiation of muscle precursor cells into a brown fat cell lineage (Seale et al. 2008), in part through interaction with CtBP (Seale et al. 2007). The fact that BMP-7 regulates brown fat cell differentiation through up-regulation of *PRDM16* (Tseng et al. 2008) further supports the association between *PRDM16* and BMP signaling. In a recent paper, Kinameri, *et al.* examined the expression of several members of the PRDM gene family, including PRDM16, during mouse neurogenesis (Kinameri et al. 2008). They describe a brain expression pattern for PRDM16 very similar to what we have observed and reported here.

One of the hallmarks of early embryonic development is rapid growth due, in part, to robust cell proliferation. The broad expression of *PRDM16* in multiple cell types, in addition to its demonstrated role in cell differentiation, as described above, supports the notion of a role for the PRDM protein in cell proliferation. Indeed, because of the association of *PRDM16* with specific cancers and similarities to MDS1/EVI1, early work focused on its role in regulating cell proliferation. Like PRDM16, MDS1/EVI is a PR-domain containing protein that results from fusion of the MDS1 gene (containing the PR-domain) to the oncogene, EVI1 (Fears et al. 1996). In addition to MDS1/EVI1 (Sood et al. 1999), EVI1 itself has been linked to myeloid malignancies (Trubia et al. 2006). It is likely that a balance between the PR-domain-positive isoforms vs. PR-domain-minus isoforms is important for the control of cell proliferation, as has been previously suggested for other PR-domain containing proteins (Nucifora et al. 2006). Two isoforms of *PRDM16* have been reported, with a shorter variant missing most of the PR domain. Aberrant expression of this variant may lead to myelodysplastic syndrome, suggesting that the PR-domain confers tumor suppressive activity (Xiao et al. 2006). We were unable to distinguish between the two isoforms of *PRDM16* in our *in situ* hybridization analyses. Evi1 has been shown to interact with several proteins such as Smad3, GATA1, HDAC, P/CAF, JNK, CBP, and CtBP that are involved in transcriptional regulation (Wieser 2007). Based on sequence conservation, it is possible that *PRDM16* binds a similar repertoire of proteins.

Given the similarity of the PR domain to the SET domain found in histone methyltransferases, it is also possible that *PRDM16* may modulate epigenetic control of gene transcription. This adds another layer of complexity to the possible roles for this protein. The identification of both upstream effectors and downstream targets are necessary to provide clarification of the specific role of *PRDM16* in modulation of developmental signaling pathways, and tissue homeostasis.

In summary, the results reported in this study represent the first to describe the temporal and spatial expression of *PRDM16* in the developing murine embryo and are an important first step towards unraveling the functional roles for this protein.

Acknowledgments

This work was supported in part by PHS grants HD53509 and DE018215 to RMG, AA13205 to MMP, and a COBRE grant (P20RR017702) from the National Center for Research Resources. Additional support was provided by the Commonwealth of Kentucky Research Challenge Trust Fund and grant to DRW from the Kentucky Science and Engineering Foundation.

REFERENCES

Bjork, BC.; Vieira, AR.; Faust, S.; Camper, SA.; Murray, JC.; Beier, DR. Phenotypic, Genetic, and Developmental Characterization of CPO1, a Recessive ENU-induced Mouse Model of Cleft Palate. Mouse Molecular Genetics Cold Spring Harbor Press; Woodbury, NY: 2006. p. 27

Buyse I, Shao G, Huang S. The retinoblastoma protein binds to RIZ, a zinc-finger protein that shares an epitope with the adenovirus E1A protein. Proc Natl Acad Sci U S A 1995;92:4467–4471. [PubMed: 7538672]

Fears S, Mathieu C, Zeleznik-Le N, Huang S, Rowley JD, Nucifora G. Intergenic splicing of MDS1 and EVI1 occurs in normal tissues as well as in myeloid leukemia and produces a new member of the PR domain family. Proc Natl Acad Sci U S A 1996;93:1642–1647. [PubMed: 8643684]

Kajimura S, Seale P, Tomaru T, Erdjument-Bromage H, Cooper MP, Ruas JL, Chin S, Tempst P, Lazar MA, Spiegelman BM. Regulation of the brown and white fat gene programs through a PRDM16/CtBP transcriptional complex. Genes and Dev 2008;22:1397–1409. [PubMed: 18483224]

Keller AD, Maniatis T. Identification and characterization of a novel repressor of beta-interferon gene expression. Genes Dev 1991;5:868–879. [PubMed: 1851123]

Kinameri E, Inoue T, Aruga J, Imayoshi I, Kageyama R, Shimogori T, Moore AW. Prdm proto-oncogene transcription factor family expression and interaction with the Notch-Hes pathway in mouse neurogenesis. PLoS ONE 2008;3:e3859. [PubMed: 19050759]

Lahortiga I, Agirre X, Belloni E, Vazquez I, Larrayoz MJ, Gasparini P, Lo Coco F, Pelicci PG, Calasanz MJ, Odero MD. Molecular characterization of a t(1;3)(p36;q21) in a patient with MDS. MEL1 is widely expressed in normal tissues, including bone marrow, and it is not overexpressed in the t(1;3) cells. Oncogene 2004;23:311–316. [PubMed: 14712237]

Mochizuki N, Shimizu S, Nagasawa T, Tanaka H, Taniwaki M, Yokota J, Morishita K. A novel gene, MEL1, mapped to 1p36.3 is highly homologous to the MDS1/EVI1 gene and is transcriptionally activated in t(1;3)(p36;q21)-positive leukemia cells. Blood 2000;96:3209–3214. [PubMed: 11050005]

Nishikata I, Sasaki H, Iga M, Tateno Y, Imayoshi S, Asou N, Nakamura T, Morishita K. A novel EVI1 gene family, MEL1, lacking a PR domain (MEL1S) is expressed mainly in t(1;3)(p36;q21)-positive AML and blocks G-CSF-induced myeloid differentiation. Blood 2003a;102:3323–3332. [PubMed: 12816872]

Nishikata I, Sasaki H, Iga M, Tateno Y, Imayoshi S, Asou N, Nakamura T, Morishita K. A novel EVI1 gene family, MEL1, lacking a PR domain (MEL1S) is expressed mainly in t(1;3)(p36;q21)-positive AML and blocks G-CSF-induced myeloid differentiation. Blood 2003b;102:3323–3332. [PubMed: 12816872]

Nucifora G, Laricchia-Robbio L, Senyuk V. EVI1 and hematopoietic disorders: history and perspectives. Gene 2006;368:1–11. [PubMed: 16314052]

Seale P, Bjork BC, Yang W, Kajimura S, Chin S, Kuang S, Scime A, Devarakonda S, Conroe HM, Erdjument-Bromage H, Tempst P, Rudnicki MA, Beier DR, Spiegelman BM. PRDM16 controls a brown fat/skeletal muscle switch. Nature 2008;454:961–967. [PubMed: 18719582]

Seale P, Kajimura S, Yang W, Chin S, Rohas LM, Uldry M, Tavernier G, Langin D, Spiegelman BM. Transcriptional control of brown fat determination by PRDM16. Cell Metab 2007;6:38–54. [PubMed: 17618855]

Shing DC, Trubia M, Marchesi F, Radaelli E, Belloni E, Tapinassi C, Scanziani E, Mecucci C, Crescenzi B, Lahortiga I, Odero MD, Zardo G, Gruszka A, Minucci S, DiFiore PP, Pelicci PG. Overexpression of sPRDM16 coupled with loss of p53 induces myeloid leukemias in mice. J. Clin. Invest 2007;117:3696–3707. [PubMed: 18037989]

Sood R, Talwar-Trikha A, Chakrabarti SR, Nucifora G. MDS1/EVI1 enhances TGF-beta1 signaling and strengthens its growth-inhibitory effect but the leukemia-associated fusion protein AML1/MDS1/EVI1, product of the t(3;21), abrogates growth-inhibition in response to TGF-beta1. Leukemia 1999;13:348–357. [PubMed: 10086725]

Trubia M, Albano F, Cavazzini F, Cambrin GR, Quarta G, Fabbiano F, Ciambelli F, Magro D, Hernandezo JM, Mancini M, Diverio D, Pelicci PG, Coco FL, Mecucci C, Specchia G, Rocchi M, Liso V, Castoldi G, Cuneo A. Characterization of a recurrent translocation t(2;3)(p15–22;q26) occurring in acute myeloid leukaemia. Leukemia 2006;20:48–54. [PubMed: 16619048]

Tseng YH, Kokkotou E, Schulz TJ, Huang TL, Winnay JN, Taniguchi CM, Tran TT, Suzuki R, Espinoza DO, Yamamoto Y, Ahrens MJ, Dudley AT, Norris AW, Kulkarni RN, Kahn CR. New role of bone morphogenetic protein 7 in brown adipogenesis and energy expenditure. Nature 2008;454:1000–1004. [PubMed: 18719589]

Van Campenhout C, Nichane M, Antoniou A, Pendeville H, Bronchain OJ, Marine JC, Mazabraud A, Voz ML, Bellefroid EJ. Evi1 is specifically expressed in the distal tubule and duct of the Xenopus pronephros and plays a role in its formation. Dev. Biol 2006;294:203–219. [PubMed: 16574097]

Warner DR, Horn KH, Mudd L, Webb CL, Greene RM, Pisano MM. PRDM16/MEL1: A novel Smad binding protein expressed in murine embryonic orofacial tissue. Biochim Biophys Acta 2007;1773:814–820. [PubMed: 17467076]

Wieser R. The oncogene and developmental regulator EVI1: expression, biochemical properties, and biological functions. Gene 2007;396:346–357. [PubMed: 17507183]

Xiao Z, Zhang M, Liu X, Zhang Y, Yang L, Hao Y. MEL1S, not MEL1, is overexpressed in myelodysplastic syndromes patients with t(1;3)(p36;q21). Leuk. Res 2006;30:332–334. [PubMed: 16102824]

Yoshida M, Nosaka K, Yasunaga J, Nishikata I, Morishita K, Matsuoka M. Aberrant expression of the MEL1S gene identified in association with hypomethylation in adult T-cell leukemia cells. Blood 2004;103:2753–2760. [PubMed: 14656887]

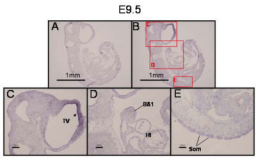

Figure 1. Expression of *PRDM16* in the E9.5 mouse embryo

Fixed, frozen E9.5 embryos were sectioned and subjected to *in situ* hybridization with a *PRDM16*-specific riboprobe. A) *PRDM16* sense riboprobe negative control. B) *PRDM16* antisense riboprobe. Lettered red boxes in panel B indicate areas shown in higher magnification in panels C–E. C) *PRDM16* was predominately expressed in the neuroepithelial lining of the telencephalic vesicle (TV, arrowhead). D) Expression was also detected in the first branchial arch (BA1) and in the dorsal aspect of the somites (Som) (panel E). Ht, heart. Scale bar = 1 mm in panels A and B and 100 μm in panels C–E. Panel E was taken from a section adjacent to the one presented in panel B.

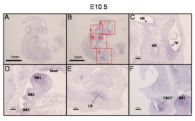

Figure 2. Expression of *PRDM16* in the E10.5 mouse embryo

A,B) *In situ* hybridization with *PRDM16* sense or antisense riboprobe, respectively (low magnification, 20X). Lettered red boxes in panel B indicate areas shown in higher magnification in panels C–F (100X). C) Similar to E9.5, expression of *PRDM16* was detected in the neuroepithelium lining telencephalic vesicle (TV, arrowhead). (Note: the circle within the TV in panel C is an artifact (air bubble)). Expression of *PRDM16* was also detected in the neuroepithelium of the hindbrain (HB, arrowhead) and in the optic stalk (OS). D) Notable expression of *PRDM16* was seen in the first, second and third branchial arches (BA1, BA2, BA3) and in the epithelium of the stomadeal roof (Stom). *PRDM16* was expressed in the developing lung bud (LB, panel E) and in the facio-acoustic preganglion complex (FAPC, panel F). Scale bar = 1 mm in panel A and B and 100 μm in panels C–F.

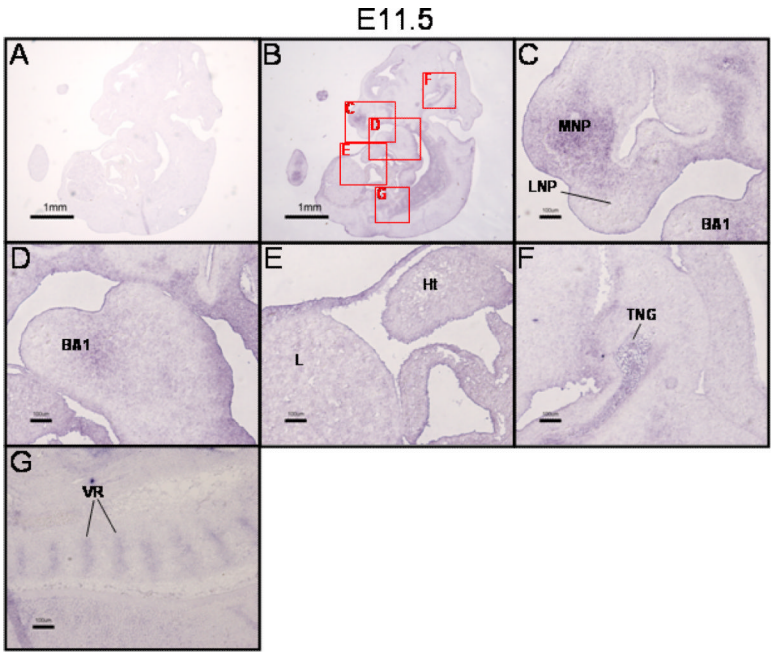

Figure 3. *PRDM16* expression in the E11.5 mouse embryo

A) *In situ* hybridization of sagittal sections of an E11.5 mouse embryo with a *PRDM16* sense riboprobe (negative control) demonstrating the extent of background staining. B) A section similar to that shown in panel A probed with a *PRDM16* antisense probe revealing staining in multiple tissues. Lettered boxes in panel B indicate areas shown in higher magnification in panels C–G. *PRDM16* expression was detected in the medial nasal process (MNP) and the first branchial arch (BA1) (panels C and D). Expression was also detected in the liver (L) and heart (Ht) (panel E), as well as in the ganglion of the trigeminal nerve (TNG, panel F), and vertebral region (VR, panel G). Scale bar = 1 mm in panels A and B and 100 μm in panels C–G.

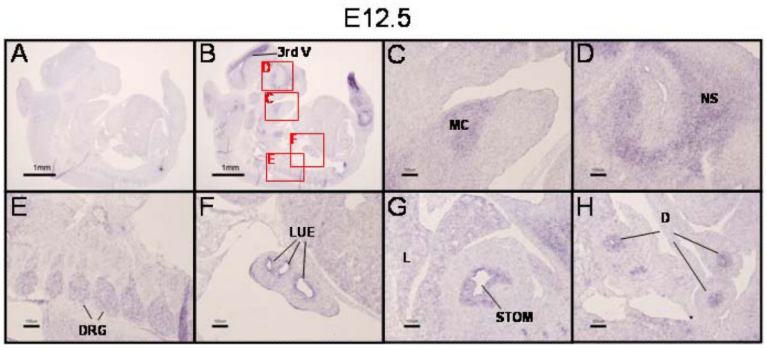

Figure 4. *PRDM16* is expressed in multiple tissues on E12.5

A,B) *In situ* hybridization with *PRDM16* sense or antisense riboprobe, respectively. Lettered boxes in panel B indicate areas shown in higher magnification in panels C–H. On E12.5 *PRDM16* was still expressed in the neuroepithelium lining the third ventricle (3rd V, panel B). In addition, *PRDM16* is expressed in Meckel's cartilage (MC, panel C), the nasal septum (NS, panel D), dorsal root ganglia (DRG, panel E) and lung epithelium (LUE, panel F). Expression is now also seen in the developing gastrointestinal system in the stomach (STOM, panel G) and duodenum (D, panel H). Panels G and H were photographed from sections adjacent to that presented in panel B in order to demonstrate expression of PRDM16 in the developing gut. Scale bar = 1 mm in panels A and B and 100 μm in panels C–H.

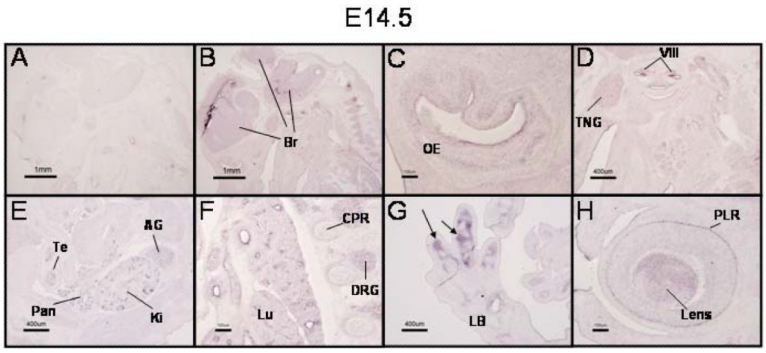

Figure 5. Broad expression of *PRDM16* in E14.5 mouse embryos

In situ hybridization of sagittal sections of an E14.5 mouse embryo with a *PRDM16* sense (A) and antisense (B–H) riboprobes. Expression of *PRDM16* during this stage of development encompasses multiple tissues including widespread signals in the developing brain (Br, panel B) and olfactory epithelium (OE, panel C). Panel D demonstrates expression of *PRDM16* in the trigeminal ganglion (TNG), the vestibulocochlear ganglion (VIII), and submandibular glands (SMG). Expression was also observed in the developing testis (Te), pancreas (Pan), kidney (Ki) and adrenal gland (AG) (panel E). The developing lung (Lu) also expressed *PRDM16* as well as the dorsal root ganglia (DRG) and cartilage primordia of the ribs (CPR) (panel F). In the hindlimb, *PRDM16* expression was restricted to the perichondrium surrounding the developing tarsal bones (panel G, arrows). Expression was detected in the eye in the pigment layer of the retina (PLR) and in the lens (Lens, panel H). Scale bars: panels A and B = 1 mm; C, F, and H = 100 μm; and D, E, and G = 400 μm.